Numerical Investigation on the Performance of Concrete-Filled Double-Skin Tube Columns Under Blast Loading

Abhimanyu U, H M Jagadisha and Pratheeksha

Abstract— **In recent years, Concrete-Filled Double-Skin Tube (CFDST) columns have become a promising structural system, demonstrating improved strength, ductility, and sustainability when compared to conventional column designs. CFDST columns comprise two steel tubes placed concentrically infilled with concrete. Square and circular hollow steel sections are commonly used in CFDST. The higher strength-to-weight ratio is a primary factor in preferring CFDST columns over Concrete-Filled Steel Tube (CFST) columns. In this study, a circular CFDST column is modeled and validated using the Finite Element Analysis-based software ABAQUS. The response of the CFDST column under blast loading is explored. The influence of variables such as axial loading, outer steel tube thickness, hollowness ratio, angle of incidence, and scaled distance on blast resistance is determined through the parametric study. The study also explores the effectiveness of the introduction of steel reinforcement in the concrete infill of the CFDST column for enhancement of blast resistance. The results highlight that increasing the outer steel tube thickness and incorporating steel reinforcement lead to an enhanced blast resistance of structures. However, the study does not find definitive evidence indicating that the hollowness ratio affects the behavior of the CFDST column.**

Index Terms— **Angle of incidence, blast loading, CFDST, concrete damaged plasticity, finite element analysis, scaled distance.**

I. Introduction

In recent years, the increasing threats and terrorist activities around the world demand the need for the safety and resilience of buildings against the damage caused by accidental loads. Designing structures with enhanced blast resistance is crucial, and an essential need for important buildings such as the military, public buildings, bridges, and pipelines. Exposure of the structure to the rapid release of energy in the form of shock waves causes significant damage to the load-bearing component of the building and structural members. The sudden failure of the column and structural members will hinder the integrity of the structure.

Manuscript received August 30, 2023; revised April 04, 2024.

Abhimanyu U is an Assistant Professor in the Department of Civil Engineering, Manipal Institute of Technology, Manipal Academy of Higher Education, Manipal, 576104, India (e-mail: abhimanyu.u@manipal.edu).

H M Jagadisha is an Assistant Professor in the Department of Civil Engineering, Manipal Institute of Technology, Manipal Academy of Higher Education, Manipal, 576104, India (corresponding author; phone: +91 9164270703; e-mail: jagadisha.hm@manipal.edu).

Pratheeksha is a postgraduate student in the Department of Civil Engineering, Manipal Institute of Technology, Manipal Academy of Higher Education, Manipal, 576104, India (e-mail: pratheeksha.96.pb@gmail.com).

CFST columns are composite structures commonly used in bridge piers, high-rise buildings, and load-bearing structures for their improved performance, durability, and seismic performance. The influence of the thickness of the steel tube, charge weight, and cross-section of CFST columns on the blast resistance shows better resistance than conventional structures, in addition circular steel tube sections provide better concrete confinement than square steel tubes which are prone to local buckling under blast load [4], [5].

Numerical analysis, simulations, and an assessment of performance were conducted to examine structural resistance to blasts under different loads and exposure to fire. The LS-DYNA and ABAQUS results reveal that infill concrete confinement prevents local buckling of the steel tube when subjected to blast loads. Additionally, the findings suggest that increasing the thickness of the steel tube enhances the column resistance to blasts. The duration of the fire was found to be influential in the emergence of cracks due to blast loads hence need a new concrete damage plasticity model with the effects of high temperature and high strain rate [6]–[9].

Concrete-Filled Double-Skin Tubular (CFDST) members typically display higher strength and deformation capabilities. Additionally, various studies have showcased the remarkable seismic ductility and energy dissipation potential inherent in CFDST members [10]-[12]. Exploring the effectiveness of CFDST columns in comparison to CFST columns through numerical simulation revealed that, despite he weight-to-strength advantages of CFDST structural elements, the axial capacity of CFST columns was found to be higher than the CFDST columns [13]. The higher blast resistance and remarkable ductility of CFDST columns have been showcased when subjected to close-in blast loading through experimental study [14]. CFDST columns display a higher residual axial load-carrying capacity in comparison to Reinforced Concrete members under contact explosions [15], [16]. From numerical model results on evaluating the post-blast residual stress of CFDST under a close-in blast, an empirical formula is proposed to predict the residual axial load-bearing capacity [17]. CFDST Results from experimental work on ultra-high-performance CFDST columns subjected to close-in blast loading reveal that no apparent buckling or ruptures were observed in the steel tubes. Upon removal of the external steel tube, only minor cracks detected in the core concrete [14]. The comparison of a circular CFDST column with a dodecagonal CFDST column resolved that the circular steel tube confinement

effect is better than dodecagonal tubes [18]. The CFDST column exposed to blast loads, both close-in and contact detonation scenarios reveal that the primary function of the external steel is to effectively counteract concrete core spalling. Meanwhile, the concrete core significantly contributes to absorbing and dispersing the energy imparted by the explosive impact [19], [20].

As the demand for efficient and resilient structural solutions continues to grow, CFDST columns represent a promising avenue for research and application. The present study focuses on a comprehensive investigation into the response of CFDST columns subjected to blast loading. The analysis will be done using the ABAQUS software, a powerful FEA tool. The study aims to investigate various parameters that influence the effectiveness of CFDST columns when exposed to close-in blast loading scenarios. The effectiveness of the steel reinforcement along with the CFDST column under blast loading is also examined.

II. MODELLING AND SIMULATIONS

In the present study, using the ABAQUS software a FEA model of CFDST is generated under blast loading and the simulated model is validated using the strain compatibility theory.

A. Element type

The inner steel tube, outer steel tube, concrete core, loading plate, and steel reinforcement are modeled in the software. Eight-node solid brick elements (C3D8R) with reduced integration and hourglass control are adapted to simulate the steel tubes and the concrete core. The loading plate is modeled as a rigid element that can be set in the interaction module. The element B31 used to model steel reinforcement is described as the linear beam in space. The specifications of the steel tubes are opted for considering their commercial availability and the dimensions of the steel tubes adopted in this study are detailed in Table 1. The typical cross-section of the CFDST along with the ABAQUS meshed assembly model of the CFDST column is shown in Figure 1 and Figure 2.

The specifications of the steel tubes are opted for considering their commercial availability and their dimensions used in the research are listed in Table 1.

B. Blast load

The blast load can be classified as close-range, near-field, and far-field blast loading based on its scaled distances.

- Close-range blast z < 1.2 m/kg$^{1/3}$.
- Near-field blast 1.2 < z <3.97 m/kg$^{1/3}$.
- Far-field blast z > 3.97 m/kg$^{1/3}$.

The prevention of near-field and far-field blast loads is possible with proper planning of the building layout and the provision of blast barriers. However, it is tedious in the case of a close-range blast loading. Therefore, the systematic study of the behavior of the structure under close-range blast load is essential.

Blast load is dynamically applied on the outer surface of the column and is defined as an incident wave in the interaction property. The weight of equivalent TNT 9 kg was inputted at the interaction along with the source of the charge. The source of the charge was at a distance 0.42m from the outer surface of the CFDST column which accounts for a scaled distance of 0.5 (ft/lb$^{1/3}$). The software assumes the shape of the charge as spherical. An axial load of 1500 kN is applied along with the blast load.

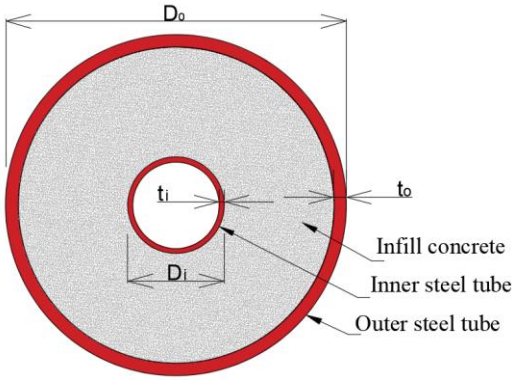

Fig. 1. Typical cross-section details of the CFDST column

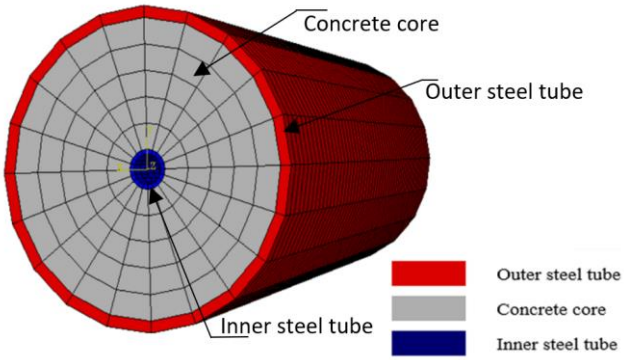

Fig. 2. ABAQUS meshed assembly of the CFDST column

TABLE I
SPECIFICATION OF THE STEEL TUBES

Specification	Value
Outer steel tube diameter (D_o)	219.1 mm
Outer steel tube thickness (t_o)	8.0 mm
Inner steel tube diameter (D_i)	26.9 mm
Inner steel tube thickness (t_i)	3.2 mm

C. Interactions

The interaction module of the software was used to establish the contact connection between the infill concrete and the steel tubes. Normal and tangential behaviors were used to describe the contact in the interaction property. The pressure developed and the friction between the surfaces are defined in normal and tangential behavior respectively. The hard contact option ensures no contact pressure developed between the surfaces and the friction coefficient value adopted was 0.3. In the interaction between the infill concrete and the outer steel tube, the outer steel tube is defined as the master surface, and the concrete core as the slave surface. Conversely, for the interaction between the inner steel tube and the concrete core, the roles are reversed: the concrete core is designated as the master surface, while the inner steel tube serves as the slave surface

The contact between the column components and the loading plate is created in the tie constraint, where the loading plate and surface of the column are assigned as the master surface and the slave surface respectively. Steel reinforcement is labeled as an embedded region and the

concrete core as the host region. Thus, the embedded region constraint feature is employed to define the connection between the steel reinforcement and the concrete core.

D. Mesh

The meshing of the element should be such that the hourglass effect and the over-stiff locking should be eliminated. The element type used to mesh each component is mentioned earlier. The steel tube mesh includes 20, 1, and 60 elements along the circumference, radius, and length respectively. The concrete core mesh includes 20, 5, and 60 elements along the circumference, radius, and length respectively as shown in Figure 2. The longitudinal and transverse reinforcement mesh includes 60 and 20 elements respectively.

E. Material properties

The compatibility of the grades of the concrete and steel is the basis for the selection of the materials. Choose materials in a way that ensures the external steel tube undergoes yielding before the concrete experiences its maximum stress. If the yield strain of the external steel tube (ε_y) is lower than the strain associated with the peak stress of the concrete (ε_c), the material grades of the steel tubes and the infill concrete are said to be compatible.

Steel

The stress-strain model proposed by [21], [22] which is the five-stage stress-strain curve is used to model the behavior of steel tubes. The true stress-strain curve is inputted in the ABAQUS software and the conversion of the nominal stress-strain values to true stress-strain is done in the material module. Young's modulus and Poisson's ratio adopted for steel is 196000 N/mm^2 and 0.3 respectively. Fe310 grade of steel was adopted for the steel tubes. The stress-strain curve used to represent the steel tube is shown in Figure 3.

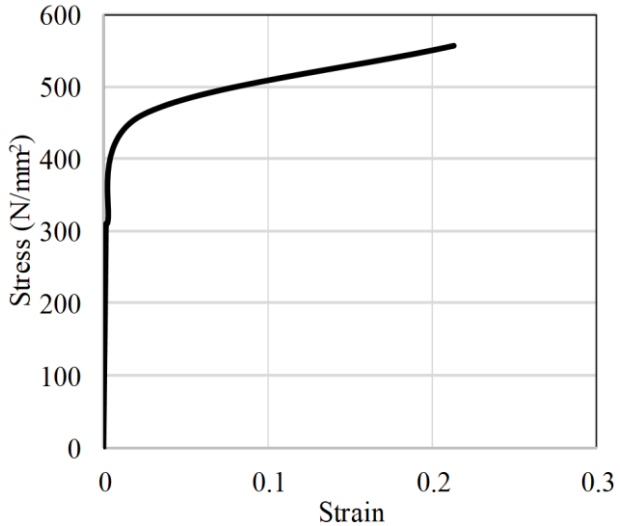

Fig. 3. Stress-strain model for the steel tubes

Concrete core

The constitutive model proposed by [23] is utilized to define the behavior of the concrete core. Equation (1) is used to represent the compressive stress-strain relationship.

$$y = \begin{cases} 2x - x^2, & x \le 1 \\ x/\beta o(x-1)^2 + x, & x > 1 \end{cases} \quad (1)$$

In (1), if $x=\varepsilon/\varepsilon_0$ and $y=\sigma/f_c'$; σ and ε are the stress and strain in the concrete core respectively. f_c' is the concrete strength and ε_0 is the strain at maximum stress in the concrete which is computed using (2).

$$\varepsilon_o = \varepsilon_c + 800.\xi^{0.2}.10^{-6} \quad (2)$$

The parameters ε_c, β_0, and ξ can be calculated using (3), (4) and (5).

$$\varepsilon_c = (1300 + 12.5\,.f_c').10^{-6} \quad (3)$$

$$\beta_o = 0.5\,.((2.36\times10^{-5})^{(0.25+(\xi-0.5))})^7 f_c'^{\,0.5} \quad (4)$$

$$\beta_o \ge 0.12 \quad (5)$$

$$\xi = \frac{A_{so}\,.\,f_y}{A_c\,.\,f_{ck}} \quad (6)$$

where ξ is the confinement factor, f_y and A_{so} are the yield strength and the cross-section area of the steel tube respectively. A_c and f_{ck} are the area of cross-section and the compressive strength of the concrete core respectively.

The software provides the capability of simulating the damage of the concrete core using three models i.e. smeared crack model, the brittle crack model, and the concrete damage plasticity that exists in the material library. The concrete damage plasticity predicts two failure mechanisms in concrete, tensile cracking, and compression crushing. The input required for the compression behavior simulation is stress (σ_c), inelastic strain (ε_c^{in}), and damage parameter (d_c) while the input required for the tensile behavior is stress (σ_t), cracking strain (ε_t^{ck}), and damage parameters (d_t). The grade of concrete used is M60. The compressive stress-strain model for the concrete core is shown in Figure 4.

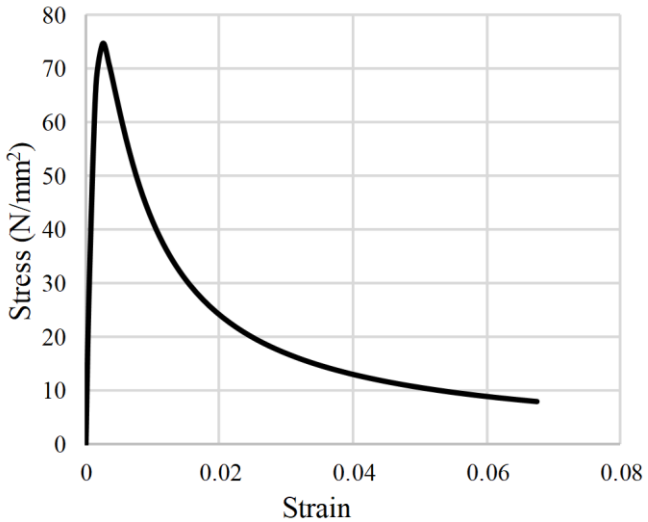

Fig. 4. Stress-strain model for the concrete core

The values assigned are 30 degrees for the dilation angle, 0.1 for eccentricity, 1.16 for the ratio of compressive strength under biaxial loading to uniaxial loading, 0.6667 for the invariant stress ratio, and 0.0005 for the viscosity parameter [21]. The viscosity parameter is taken as 0.0005 since the software accepts only non-zero values. The Young's modulus and Poisson's ratio values used are

$4730\sqrt{(f_c')}$ and 0.2 respectively [21].

TABLE 2
VARIABLES USED IN THE PARAMETRIC STUDY

Variable	Value
Axial load	1000 kN
	1500 kN
	2000 kN
Outer steel tube thickness	6 mm
	8 mm
	10 mm
Hollowness ratio	0.10
	0.13
	0.16
Scaled distance	0.5
	0.7
	0.9
Angle of incidence	20°
	50°
	80°
	90°
Steel reinforcement	Longitudinal reinforcement: 6 bars of 16 mm diameter
	Transverse reinforcement: 10 mm diameter at 150 mm center-to-center.

F. Parametric study

The geometric parameters of the CFDST column and the blast load parameters are used to study their influence on the response of the CFDST column subjected to blast loading. The parameters used in the study are axial load, outer steel tube thickness, hollowness ratio, scaled distance, angle of incidence, and provision of steel reinforcement. These parameters are selected for the study to simulate a realistic scenario of a blast where it can occur at any distance away from the column and position above the ground with various weights of charges. All these three parameters are represented by scaled distance and angle of incidence. The effect of steel reinforcement is included in the study since in several standard codes of practice the minimum steel is mandated for fire resistance of CFDST. The values of the parameters are shown in Table 2.

Fifteen models incorporating the parameters are modeled in the software and the response of the CFDST column is noted down.

III. RESULTS AND DISCUSSION

A. Response of the CFDST column subjected to blast loading

Under the blast loading the compressive damage occurring in the CFDST column is depicted in Figure 5. The maximum compressive damage occurs in the elements close to the source of detonation. The variation of the compressive damage from the ABAQUS interface in one of those elements is shown in Figure 5. The maximum compressive damage in the CFDST column is 0.436. This is obtained from compression damage parameters corresponding to inelastic stress-strain results obtained. This is obtained from the DAMAGEC results output in the software. Localized dents are formed on the surface of the CFDST column when exposed to close-in blast loading.

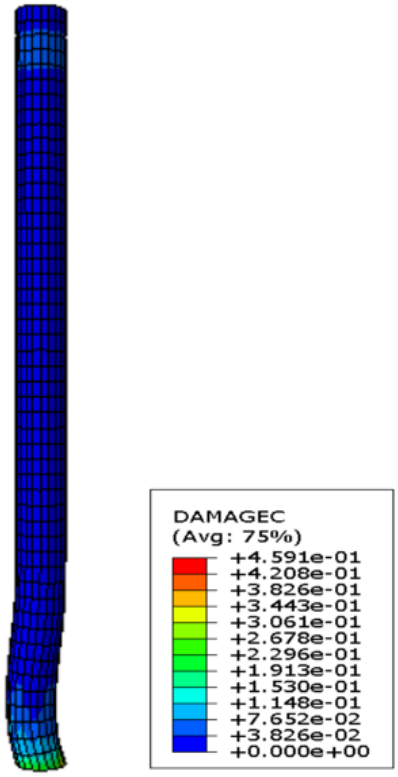

Fig. 5. Compressive damage results of the CFDST column obtained using DAMAGEC output

B. Results of parametric study

Effect of axial load

The Von Mises stress acting on the CFDST column illustrates its behavior under different axial loads. Figure 11 shows the highest Von Mises stress distribution from the ABAQUS interface, developed in the column during blast loading while varying the axial load but keeping other parameters constant.

It can be seen in Figure 7 that the stress developed in the column reduces by 22.13% and 29.75% when the axial load is increased to 1500 kN and 2000 kN respectively. This demonstrates better blast resistance of the CFDST column when the axial load is increased. This is due to the improved confinement of infill concrete with the increasing axial load, provided the applied axial load is below the crippling or critical load of the column.

Effect of Outer Steel Tube Thickness

The effect of the outer steel tube thickness on the blast resistance of the CFDST column is measured in terms of Von Mises stress distribution in the column. The maximum Von Mises stress distribution acting on the CFDST column with varying outer steel tube thickness is shown in Figure 12.

Figure 8 shows the stress in CFDST columns is reduced by 3.10% and 12.76% when the outer steel tube thickness is

increased to 8 mm and 10 mm respectively. The outer steel tube surface is exposed to the blast load and it plays a key role in enhancing the blast resistance of the column. The increasing outer steel tube thickness positively affects blast resistance by the reduction in Von Mises stresses.

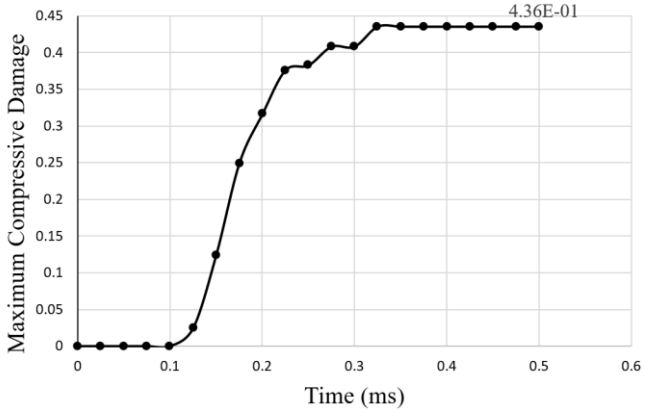

Fig. 6 Variation of compressive damage with time

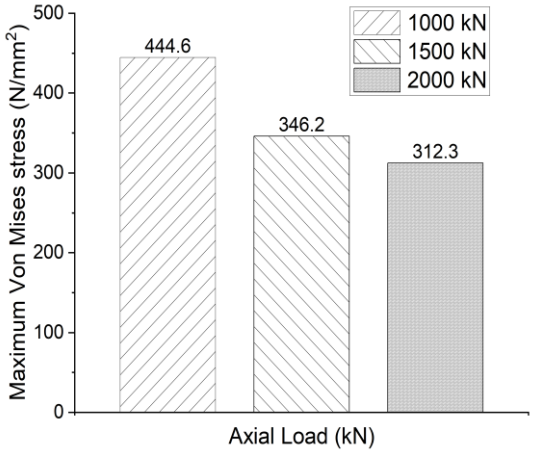

Fig. 7 Maximum Von Mises stress in the CFDST column with varying axial load

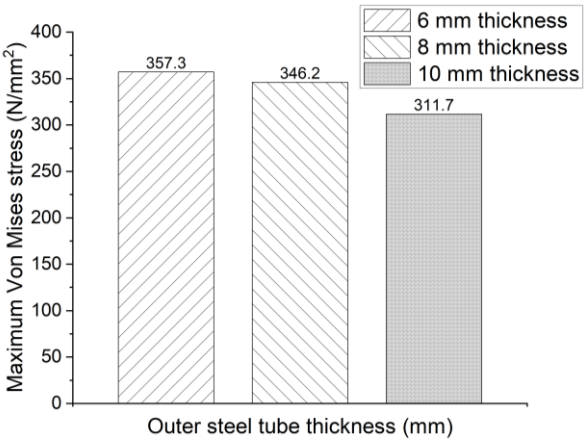

Fig. 8 Maximum Von Mises stress with varying outer steel tube thickness

Effect of hollowness ratio

The blast resistance of the CFDST column with varying hollowness ratio is represented using the von Mises stresses developed in the column. The maximum von Mises stress distribution acting on the CFDST column is shown in Figure 13.

The results from Figure 9 do not provide conclusive evidence regarding the influence of the hollowness ratio on the blast resistance of the CFDST column. However, a systematic optimization study with a wider range of hollowness ratios may be required to study the influence of the hollowness ratio on the blast resistance of the CFDST column.

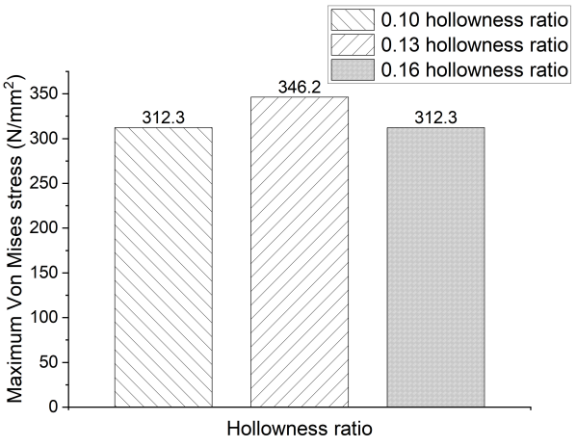

Fig. 9 Maximum Von Mises stress with varying hollowness ratio

Effect of scaled distance

The blast pressure of the incident blast wave is obtained using the IWCONWEP results output of the software. The peak reflected overpressure can be estimated using a technical manual [23]. The predicted blast pressures and the IWCONWEP results are compared for scaled distances 0.5, 0.7, and 0.9 in Figure 10, Figure 14, and Figure 15 respectively.

The value of peak overpressure is underestimated by the software for all the scaled distances studied. It may be due to the lack of simulation of the reflections of the blast waves in the software. However, the difference between the predicted peak blast pressure and IWNCONWEP peak blast pressure decreases with the increasing scaled distance. The time of arrival of the blast wave is simulated accurately when the scaled distance is 0.5 but a difference is seen in the predicted and software results of the time of arrival for scaled distances 0.7 and 0.9.

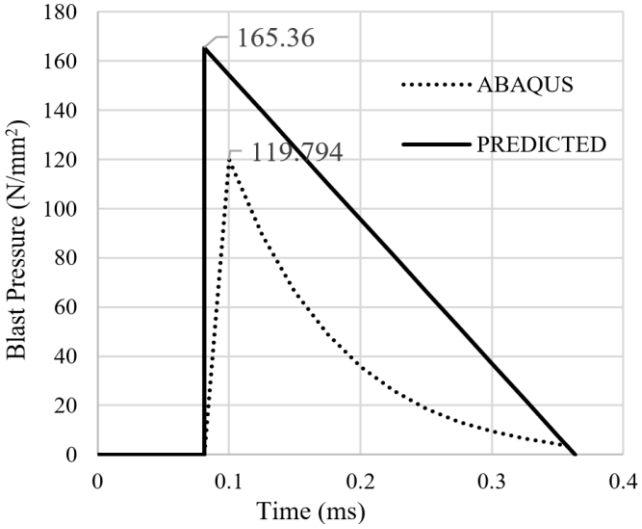

Fig. 10 Comparison of blast pressures obtained from ABAQUS and predicted values (z=0.5)

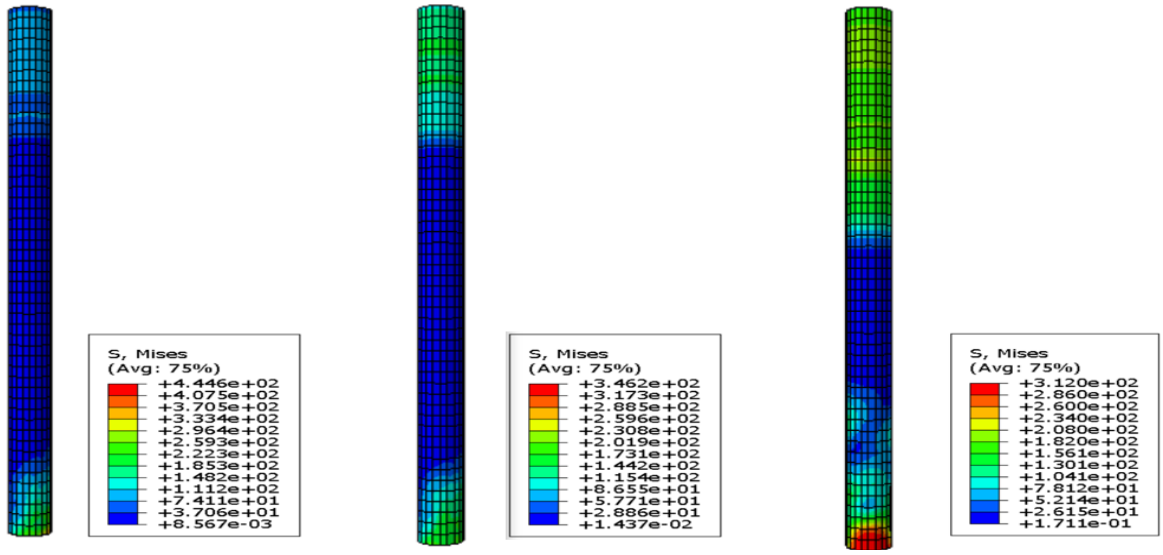

(a) (b) (c)

Fig. 11 Variation of Maximum Von Mises stress distribution in ABAQUS along CFDST column by varying axial load a) 1000 kN b) 1500 kN c) 2000 kN

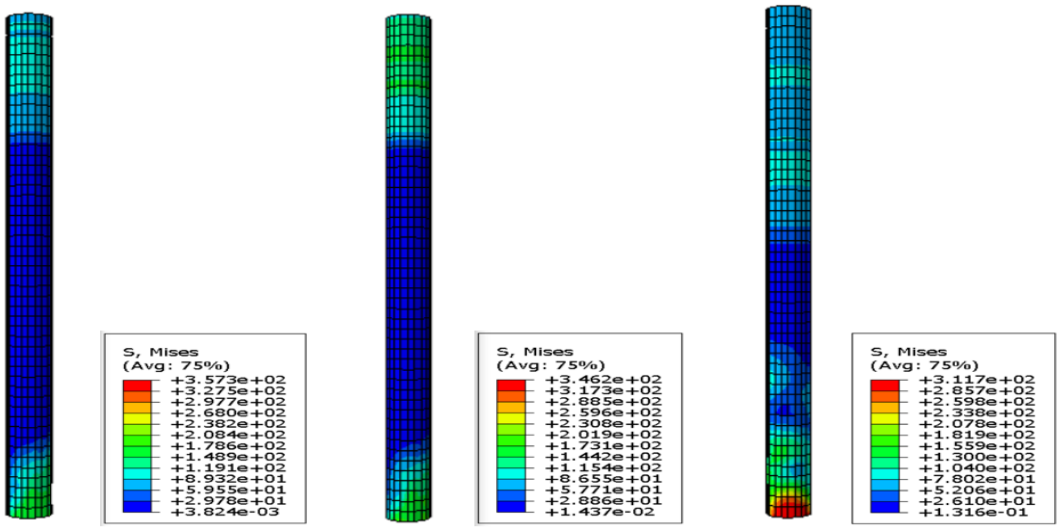

(a) (b) (c)

Fig. 12 Variation of Maximum Von Mises stress distribution in ABAQUS along CFDST column by varying outer steel tube thickness a) 6 mm b) 8 mm c) 10 mm

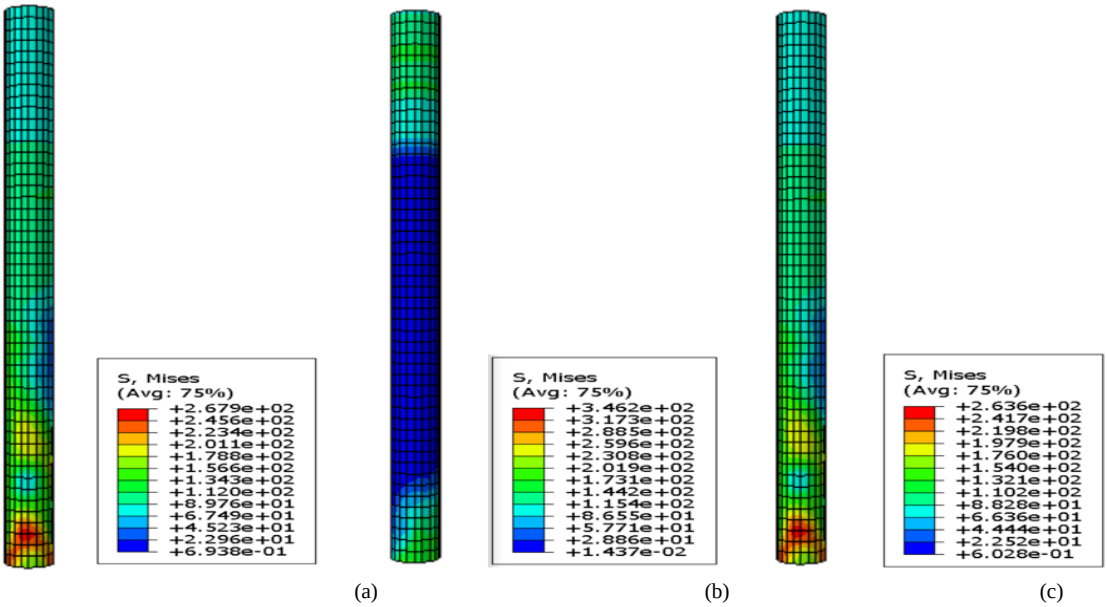

(a) (b) (c)

Fig. 13 Variation of Maximum Von Mises stress distribution in ABAQUS along CFDST column by varying hollowness ratio a) 0.1 b) 0.13 c) 0.16

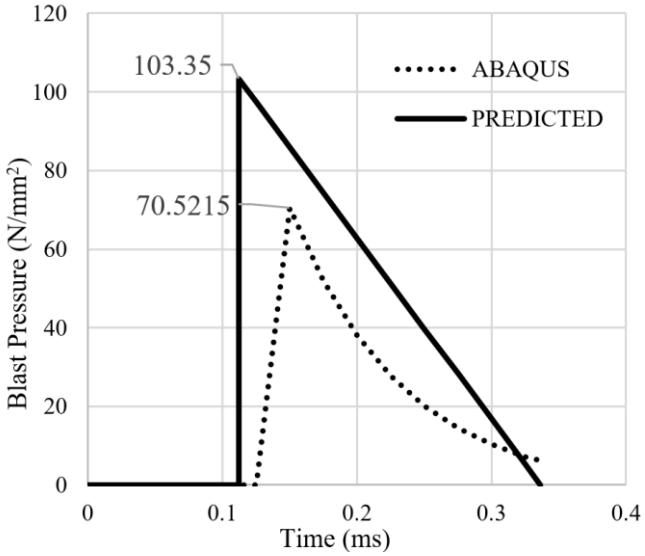

Fig. 14 Comparison of blast pressures obtained from ABAQUS and predicted values (z=0.7)

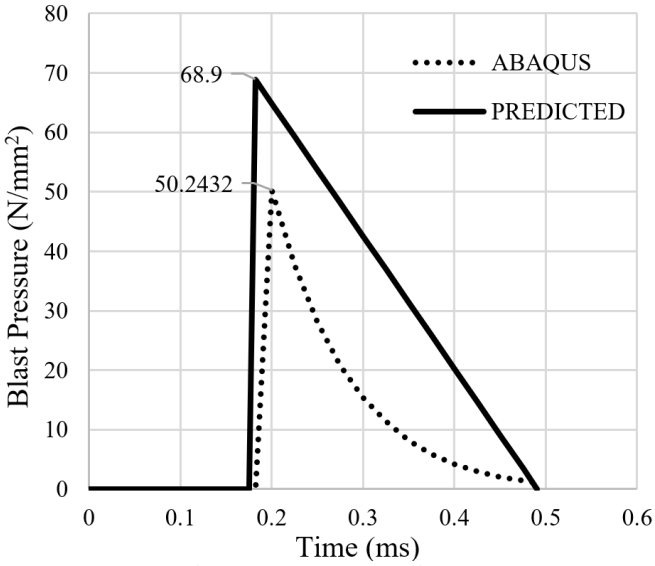

Fig. 15 Comparison of blast pressures obtained from ABAQUS and predicted values (z=0.9)

Effect of angle of incidence

The angle of incidence of the blast waves causes reflected wavefront. The interaction of reflected and incidence blast waves results in swaying of the resultant blast wave. This causes either an increase or decrease of the blast pressure on the structures. Keeping the stand-off distance constant, the height of the charge from the ground is varied with the angle of incidence. The blast pressure of the blast wave with the varying angles of incidence at the base of the column is recorded in Figure 16.

The peak overpressure of the blast wave increases with the increase in the angle of incidence. This is due to the increase in reflection of the blast wave when the height of the charge from the ground reduces. The height of the charge reduces with the increasing angle of incidence.

Effect of provision of steel reinforcement

The provision of steel reinforcement is generally for fire safety as per the codes of practice. One of the methods to enhance the blast resistance of the CFDST column is to improve the tensile behavior of the concrete core. The provision of the steel reinforcement is an attempt to enrich the tensile behavior of the concrete core and therefore increase the blast resistance of the column.

Peak Von Mises stress developed in the column with and without the provision of the steel reinforcement is shown in Figure 17.

It can be concluded that the provision of the steel reinforcement enhances the blast resistance of the CFDST column since a decrease of 9.84% in von Mises stress can be seen in the CFDST column.

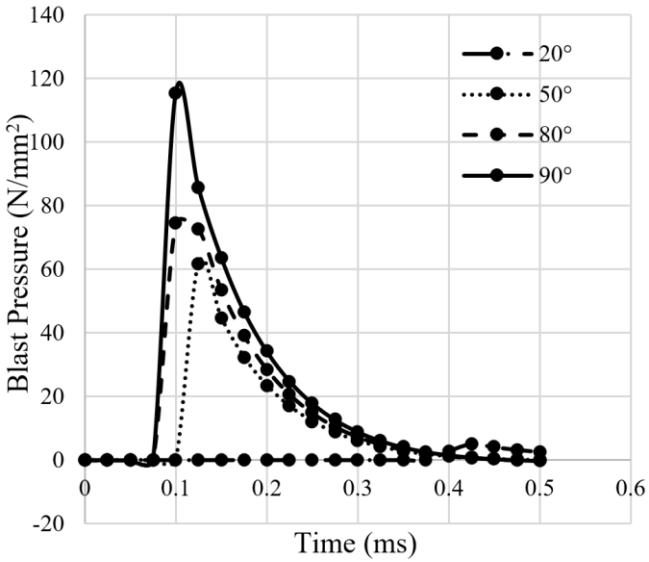

Fig. 16 Comparison of blast pressures with varying angle of incidence

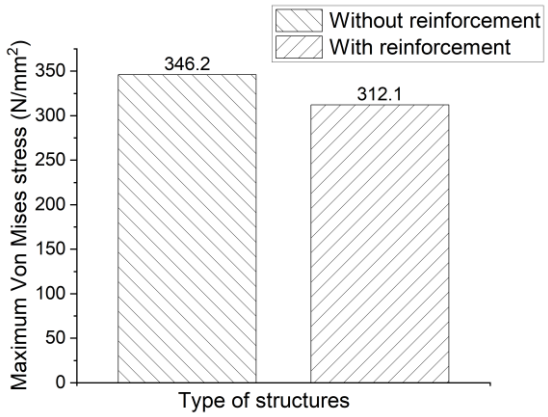

Fig. 17 Maximum Von Mises stress with the provision of steel reinforcement

IV. CONCLUSION

The performance of the CFDST column under close-in blast load is significantly impacted by the axial load-carrying capacity of the column. A reduction of 22.13% and 29.75% in the maximum von Mises stress is observed when the axial load is increased to 1500 kN and 2000 kN respectively. This is because of the surge in the confinement of the infill concrete core with increasing axial load. The CFDST column blast resistance is enhanced by increasing the thickness of the outer steel tube. When the outer steel tube thickness is raised to 8 mm and 10 mm, a decrease in the maximum von Mises stress is observed by 3.10% and 12.76%, respectively.

The study does not find any conclusive observations to

understand the impact of the hollowness ratio on the behavior of the CFDST column. Initially stress increased with the hollowness ratio, however, stress reduced as the hollowness ratio further increased. To draw any conclusion more hollowness ratio data points, need to be considered. The control of parameters associated with the blast loading i.e. the scaled distance and the angle of incidence is tedious and calls for more detailed optimization. Their effects cannot be linearly predicted. However, the knowledge of its consequences on the functioning of the CFDST column can be vital in designing an efficient blast-resistant structural member. The implementation of steel reinforcement in the CFDST column has proven to be valuable in improving the blast resistance of the column. A stress reduction of 9.84% is seen on the CFDST column when steel reinforcement is provided.

REFERENCES

[1] Y. Liu, J. Yan, and F. Huang, "Behavior of reinforced concrete beams and columns subjected to blast loading," *Defence Technology*, vol. 14, no. 5, pp. 550–559, Oct. 2018, doi: 10.1016/j.dt.2018.07.026.

[2] S. Astarlioglu, T. Krauthammer, D. Morency, and T. P. Tran, "Behavior of reinforced concrete columns under combined effects of axial and blast-induced transverse loads," *Engineering Structures*, vol. 55, pp. 26–34, Oct. 2013, doi: 10.1016/j.engstruct.2012.12.040.

[3] H. Aoude, F. P. Dagenais, R. P. Burrell, and M. Saatcioglu, "Behavior of ultra-high performance fiber reinforced concrete columns under blast loading," *Int. J. Impact Eng*, vol. 80, pp. 185–202, Jun. 2015, doi: 10.1016/j.ijimpeng.2015.02.006.

[4] L.-H. Han and W. Li, "Seismic performance of CFST column to steel beam joint with RC slab: Experiments," *J. Constr. Steel Res.*, vol. 66, no. 11, pp. 1374–1386, Nov. 2010, doi: 10.1016/j.jcsr.2010.05.003.

[5] H. Wang, C. Wu, F. Zhang, Q. Fang, H. Xiang, P. Li, Z. Li, Y. Zhou, Y. Zhang, J. Li., "Experimental study of large-sized concrete filled steel tube columns under blast load," *Constr. Build. Mater.*, vol. 134, pp. 131–141, Mar. 2017, doi: 10.1016/j.conbuildmat.2016.12.096.

[6] C. Zhai, L. Chen, H. Xiang, and Q. Fang, "Experimental and numerical investigation into RC beams subjected to blast after exposure to fire," *Int. J. Impact Engg.*, vol. 97, pp. 29–45, Nov. 2016, doi: 10.1016/j.ijimpeng.2016.06.004.

[7] Z. Ruan, L. Chen, and Q. Fang, "Numerical investigation into dynamic responses of RC columns subjected for fire and blast," *Journal of Loss Prevention in the Process Industries*, vol. 34, pp. 10–21, Mar. 2015, doi: 10.1016/j.jlp.2015.01.009.

[8] F. Zhang, C. Wu, H. Wang, and Y. Zhou, "Numerical simulation of concrete filled steel tube columns against BLAST loads," *Thin-Walled Structures*, vol. 92, pp. 82–92, Jul. 2015, doi: 10.1016/j.tws.2015.02.020.

[9] X. Zhang, H. Hao, M. Li, Z. Zong, and J. W. Bruechert, "The blast resistant performance of concrete-filled steel-tube segmental columns," *J. Constr. Steel Res.*, vol. 168, p. 105997, May 2020, doi: 10.1016/j.jcsr.2020.105997.

[10] Q. Q. Liang, "Nonlinear analysis of circular double-skin concrete-filled steel tubular columns under axial compression," *Engineering Structures*, vol. 131, pp. 639–650, Jan. 2017, doi: 10.1016/j.engstruct.2016.10.019.

[11] K. Nakanishi, T. Kitada, and H. Nakai, "Experimental study on ultimate strength and ductility of concrete filled steel columns under strong earthquake," *J. Constr. Steel Res.*, vol. 51, pp. 297-319, 1999.

[12] Y. Zheng, C. He, and L. Zheng, "Experimental and numerical investigation of circular double-tube concrete-filled stainless steel tubular columns under cyclic loading," *Thin-Walled Structures*, vol. 132, pp. 151–166, 2018, doi: 10.1016/j.tws.2018.07.058.

[13] M. Pagoulatou, T. Sheehan, X. H. Dai, and D. Lam, "Finite element analysis on the capacity of circular concrete-filled double-skin steel tubular (CFDST) stub columns," *Engineering Structures*, vol. 72, pp. 102–112, Aug. 2014, doi: 10.1016/j.engstruct.2014.04.039.

[14] P. Fouché, M. Bruneau, and V. Chiarito, "Dual-Hazard Blast and Seismic Behavior of Concrete-Filled Double-Skin Steel Tubes Bridge Pier," *Journal of Structural Engineering*, vol. 143, no. 12, Dec. 2017, doi: 10.1061/(ASCE)ST.1943-541X.0001883.

[15] M. Li, Z. Zong, H. Hao, X. Zhang, J. Lin, and Y. Liao, "Post-blast performance and residual capacity of CFDST columns subjected to contact explosions," *J. Constr. Steel Res.*, vol. 167, p. 105960, Apr. 2020, doi: 10.1016/j.jcsr.2020.105960.

[16] M. Li, Z. Zong, G. Wu, X. Zhang, S. Yuan, and B. Tang, "Residual axial capacity of circular reinforced concrete columns subjected to contact explosions," *Advances in Structural Engineering*, vol. 25, no. 7, pp. 1622–1635, May 2022, doi: 10.1177/13694332221084028.

[17] M. Li, M. Xia, Z. Zong, G. Wu, X. Zhang, "Residual axial capacity of concrete-filled double-skin steel tube columns under close-in blast loading," *J. Constr. Steel Res.*, Volume 201, 2023, 107697, https://doi.org/10.1016/j.jcsr.2022.107697.

[18] J. Wang, X. Cheng, C. Wu, and C.-C. Hou, "Analytical behavior of dodecagonal concrete-filled double skin tubular (CFDST) columns under axial compression," *J. Constr. Steel Res.*, vol. 162, p. 105743, Nov. 2019, doi: 10.1016/j.jcsr.2019.105743.

[19] M. Li, Z. Zong, H. Hao, X. Zhang, J. Lin, and G. Xie, "Experimental and numerical study on the behaviour of CFDST columns subjected to close-in blast loading," *Engineering Structures*, vol. 185, pp. 203–220, Apr. 2019, doi: 10.1016/j.engstruct.2019.01.116.

[20] M. Li, Z. Zong, L. Liu, and F. Lou, "Experimental and numerical study on damage mechanism of CFDST bridge columns subjected to contact explosion," *Engineering Structures*, vol. 159, pp. 265–276, Mar. 2018, doi: 10.1016/j.engstruct.2018.01.006.

[21] F.-C. Wang and L.-H. Han, "Analytical behavior of special-shaped CFST stub columns under axial compression," *Thin-Walled Structures*, vol. 129, pp. 404–417, Aug. 2018, doi: 10.1016/j.tws.2018.04.013.

[22] L.-H. Han, G.-H. Yao, and Z. Tao, "Performance of concrete-filled thin-walled steel tubes under pure torsion," *Thin-Walled Structures*, vol. 45, no. 1, pp. 24–36, Jan. 2007, doi: 10.1016/j.tws.2007.01.008.

[23] L. H. Han, *Theory and practice of concrete filled steel tubular structure*, 2nd edition. Beijing Science Press, 2007.

[24] *Unified Facilities Criteria (UFC) 3-340-02, Structures to resist the effects of accidental explosions*, Department of Defense, USA, Dec. 2008.

Mr. **Abhimanyu U** received his Bachelor of Engineering (2010), and M. Tech. (2012) degrees from Visvesvaraya Technological University, Belgavi, India. At present, he is working as an Assistant Professor in the Department of Civil Engineering, Manipal Institute of Technology, MAHE, Manipal, India. His research interest includes Composite structures, FEM modelling and analysis, Precast structures, and Wavelet analysis for structural health monitoring.

Mr. **H M Jagadisha** received his Bachelor of Engineering (2009) and M. Tech. (2012) degrees from Visvesvaraya Technological University, Belgavi, India. At present, he is working as an Assistant Professor in the Department of Civil Engineering, Manipal Institute of Technology, MAHE, Manipal, India. His research interest include Composite structures, Vibration isolation structures, Interlock brick masonry, and Alkali-activated materials.

Ms. **Pratheeksha** received his Bachelor of Technology (2018) and M. Tech. (2020) degrees from Manipal Institute of Technology, MAHE, Manipal, India. At present, she is working as Assistant Engineering, in the AtkinsRéalis, Bangalore, India. Her area of interest includes Composite structures, FEM modelling and analysis, and Structural health monitoring.